

AD-A267 125



NRL/MR/6791--93-7328

Thomson Backscattered X-Rays from an Intense Laser Beam

CHA-MEI TANG

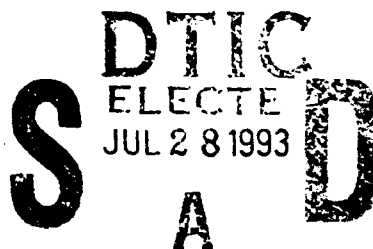
*Beam Physics Branch
Plasma Physics Division*

B. HAFIZI

*Icarus Research
Bethesda, MD*

SALLY K. RIDE

*University of California at San Diego
La Jolla, CA*



July 26, 1993

93-16855



REPORT DOCUMENTATION PAGE			Form Approved OMB No. 0704-0188	
Public reporting burden for this collection of information is estimated to average 1 hour per response, including the time for reviewing instructions, searching existing data sources, gathering and maintaining the data needed, and completing and reviewing the collection of information. Send comments regarding this burden estimate or any other aspect of this collection of information, including suggestions for reducing this burden, to Washington Headquarters Services, Directorate for Information Operations and Reports, 1215 Jefferson Davis Highway, Suite 1204, Arlington, VA 22202-4302, and to the Office of Management and Budget, Paperwork Reduction Project (0704-0188), Washington, DC 20503.				
1. AGENCY USE ONLY (Leave Blank)	2. REPORT DATE July 26, 1993	3. REPORT TYPE AND DATES COVERED Interim Report		
4. TITLE AND SUBTITLE Thomson Backscattered X-Rays from an Intense Laser Beam			5. FUNDING NUMBERS	
6. AUTHOR(S) Cha-Mei Tang, B. Hafizi,* and Sally K. Ride†				
7. PERFORMING ORGANIZATION NAME(S) AND ADDRESS(ES) Naval Research Laboratory Washington, DC 20375-5320			8. PERFORMING ORGANIZATION REPORT NUMBER NRL/MR/6791-93-7328	
9. SPONSORING/MONITORING AGENCY NAME(S) AND ADDRESS(ES) Office of Naval Research Arlington, VA 22217-5560			10. SPONSORING/MONITORING AGENCY REPORT NUMBER	
11. SUPPLEMENTARY NOTES *Icarus Research, 7113 Exfair Rd., Bethesda, MD 20814 †Department of Physics 0319, University of California at San Diego, La Jolla, CA 92093-0021				
12a. DISTRIBUTION/AVAILABILITY STATEMENT Approved for public release; distribution unlimited.			12b. DISTRIBUTION CODE	
13. ABSTRACT (Maximum 200 words) We have formulated and obtained analytical expressions for Thomson backscattered x-ray radiation for an electron beam incident on a linearly polarized electromagnetic undulator at a small angle. The analytical expressions are valid for fundamental and harmonics with arbitrarily large laser intensities. The intensity distribution pattern is evaluated numerically.				
14. SUBJECT TERMS Compton backscattering FELs Thomson backscattering x-rays			15. NUMBER OF PAGES 19	
			16. PRICE CODE	
17. SECURITY CLASSIFICATION OF REPORT UNCLASSIFIED	18. SECURITY CLASSIFICATION OF THIS PAGE UNCLASSIFIED	19. SECURITY CLASSIFICATION OF ABSTRACT UNCLASSIFIED	20. LIMITATION OF ABSTRACT UL	

CONTENTS

I. INTRODUCTION	1
II. FORMULATION	1
III. FUNDAMENTAL AND HARMONICS	6
IV. NUMERICAL RESULTS AND COMMENTS	7
ACKNOWLEDGMENTS	8
REFERENCES	9

DTIC REPORTING AND NOTED 5

Accession For	
NTIS CRA&I	<input checked="" type="checkbox"/>
DTIC TAB	<input type="checkbox"/>
Unannounced	<input type="checkbox"/>
Justification	
By	
Distribution/	
Availability Codes	
Dist	Avail and/or Special
A-1	

I. Introduction

Tunable, near monochromatic, high brightness x-rays would be an important tool in research and medical diagnostics. Synchrotron light sources have produced useful x-rays for a large user community. In this paper we examine a closely related method of x-ray generation, Thomson backscattering of x-rays from intense laser beams.¹⁻⁶ The schematic is shown in Fig. 1, where an electron beam intersects an incoming laser pulse. Radiation is backscattered at a double Doppler upshifted frequency. The laser pulse in Fig. 1 acts in a similar fashion as the static magnetic wiggler in synchrotron light sources or free electron lasers.⁷⁻¹¹

One advantage to this approach is that, because the wavelength of the laser is many orders of magnitude smaller than that of static undulators, an electron beam of much lower energy can be used to generate x-rays of a particular energy. For example, radiation of 0.04 nm wavelength (30 keV) x-rays can be generated by a laser with 1 μm wavelength and electron beam energy of 40 MeV.

An experiment is under way at Vanderbilt University to utilize the FEL as the undulator. The goal is to develop diagnostic medical imaging techniques based on the detection of atomic species important in biological substances by utilizing the discrete K-edges which are in the low keV energy range.⁴ A laser undulator has also been proposed as the damping mechanism of a very low energy (~ 1 MeV) storage ring¹² and for emittance reduction.¹³ The analytical expression of the Thomson backscattered radiation from a laser undulator derived in this paper can be applied to all these applications.

II. Formulation

We are interested in calculating the Thomson radiation intensity pattern and spectrum which results when a laser pulse intersects with an electron beam with small initial transverse momentum going in the opposite direction.

The laser pulse is assumed to be linearly polarized with frequency ω_L . The vector potential of the laser pulse can be separated into fast and slow components,

$$\mathbf{A}(\eta) = A(\eta) \sin(\eta) \hat{\mathbf{e}}_x, \quad (1)$$

where $\eta = k_L z + \omega_L t$, $k_L = \omega_L/c$. The pulse shape $A(\eta)$ and the wavenumber $k_L(\eta)$ are assumed to be a constant for the interaction time T and $\sin(\eta)$ is a fast oscillating component.

The energy radiated per unit solid angle ($d\Omega$) per unit frequency ($d\omega$) per electron is

$$\frac{d^2 I}{d\omega d\Omega} = \frac{e^2 \omega^2}{4\pi^2 c} \left| \int_{-T/2}^{T/2} dt \, \hat{n} \times (\hat{n} \times \underline{\tilde{\beta}}) \exp[i\omega(t - \hat{n} \cdot \tilde{r}/c)] \right|^2, \quad (2)$$

where \hat{n} is a unit vector pointing from the radiating electron to the observation point, \tilde{r} is the electron's coordinate, $T = L/c$ is the interaction time, L is the length of the laser pulse and $\underline{\tilde{\beta}} = c^{-1} d\tilde{r}/dt$ is the electron velocity normalized to the speed of light c . We consider an electron with small initial transverse velocity, $\beta_{x0} = v_{x0}/c$ and $\beta_{y0} = v_{y0}/c$. The symbol " \sim " above the variables denotes a function of (t).

It is convenient to use Cartesian coordinates for the velocity and position of the electrons and spherical coordinates for the Thomson backscattering radiation.⁸

$$\begin{aligned} \hat{n} \times (\hat{n} \times \underline{\tilde{\beta}}) = & -(\tilde{\beta}_x \cos \theta \cos \phi + \tilde{\beta}_y \cos \theta \sin \phi - \tilde{\beta}_z \sin \theta) \hat{e}_\theta \\ & + (\tilde{\beta}_x \sin \phi - \tilde{\beta}_y \cos \phi) \hat{e}_\phi, \end{aligned} \quad (3)$$

and

$$\hat{n} \cdot \tilde{r} = \tilde{x} \sin \theta \cos \phi + \tilde{y} \sin \theta \sin \phi + \tilde{z} \cos \theta, \quad (4)$$

where $\tilde{\beta}_x = \underline{\tilde{\beta}} \cdot \hat{e}_x$, $\tilde{x} = \tilde{r} \cdot \hat{e}_x$, and similarly for the y and z -components.

We separate the two components of the radiation

$$\frac{d^2 I}{d\omega d\Omega} = \frac{d^2 I_\theta}{d\omega d\Omega} + \frac{d^2 I_\phi}{d\omega d\Omega}, \quad (5)$$

and perform the calculation in the variable η , where

$$\frac{d^2 I_\theta}{d\omega d\Omega} = \frac{e^2 \omega^2}{4\pi^2 c^3} \left| \int_{-\Delta\eta/2}^{\Delta\eta/2} d\eta \left[\frac{\partial \tilde{x}}{\partial \eta} \cos \theta \cos \phi + \frac{\partial \tilde{y}}{\partial \eta} \cos \theta \sin \phi - \frac{\partial \tilde{z}}{\partial \eta} \sin \theta \right] \exp[i\tilde{\psi}] \right|^2, \quad (6)$$

$$\frac{d^2 I_\phi}{d\omega d\Omega} = \frac{e^2 \omega^2}{4\pi^2 c^3} \left| \int_{-\Delta\eta/2}^{\Delta\eta/2} d\eta \left[\frac{\partial \tilde{x}}{\partial \eta} \sin \phi - \frac{\partial \tilde{y}}{\partial \eta} \cos \phi \right] \exp[i\tilde{\psi}] \right|^2, \quad (7)$$

$$\tilde{\psi} = \frac{\omega}{\omega_L} \eta - \frac{\omega}{c} (\tilde{x} \sin \theta \cos \phi + \tilde{y} \sin \theta \sin \phi + \tilde{z} (1 + \cos \theta)), \quad (8)$$

$c\bar{\beta}dt = (\partial\bar{r}/\partial\eta)d\eta$, $\Delta\eta = \omega_L T = 2\pi N_o$ and N_o is the number of periods in the laser pulse.

In the 1-D limit, there are two constants of motion:

$$P_x - \frac{e}{c}A = P_{x0}, \quad (9)$$

and

$$\gamma(1 - \beta_x) = \gamma_0(1 - \beta_{x0}), \quad (10)$$

where P_x is the canonical momentum of the electron in the x-direction, and the subscript 0 denotes the initial value.¹⁴⁻¹⁶

In the following, we assume that the electron transverse motion is small, i.e., $a(\beta_{x0}^2 + \beta_{y0}^2)\gamma_x^2/2 \ll 1$, laser intensity not exceedingly large, i.e., $a \ll 2\gamma_0/\beta_{x0}$, and $k_\perp \Delta r \ll 1$, where Δr is the radius of the electron oscillation in the transverse direction driven by the laser, $a = (e/m_0 c^2)A$ and m_0 is the rest mass of the electron. The particle motions are

$$\frac{d\bar{x}}{d\eta} \simeq \frac{1}{(\omega_L/c)} \left[\bar{\beta}_{x0} - \frac{\bar{a}}{\gamma_0} \sin \eta \right], \quad (11a)$$

$$\frac{d\bar{y}}{d\eta} \simeq \frac{1}{(\omega_L/c)} \bar{\beta}_{y0}, \quad (11b)$$

and

$$\frac{d\bar{z}}{d\eta} \simeq \frac{1}{(\omega_L/c)} \left[\bar{\beta}_1 + \left(\frac{\bar{a}^2}{4\gamma_0^2} \right) (-1 + \cos(2\eta)) + \bar{\beta}_{x0} \frac{\bar{a}}{\gamma_0} \sin(\eta) \right], \quad (11c)$$

where $\beta_{x0} = (1 - \gamma_0^{-2} - \beta_{x0}^2 - \beta_{y0}^2)^{1/2}$ is the initial axial velocity, $\bar{\beta}_1 = (1 - (1 + \gamma_0^2(\beta_{x0}^2 + \beta_{y0}^2))/(\gamma_0^2(1 + \beta_{x0}^2)))/2$, $\bar{\beta}_{x0} = \beta_{x0}/(1 + \beta_{x0})$, $\bar{\beta}_{y0} = \beta_{y0}/(1 + \beta_{x0})$ and $\bar{a} = a/(1 + \beta_{x0})$. Their locations are

$$\bar{x} = \frac{1}{(\omega_L/c)} \left[\bar{\beta}_{x0} (\eta + \Delta\eta/2) + \int_{-\Delta\eta/2}^{\eta} \partial\eta' \left(\frac{\bar{a}}{\gamma_0} \right) \sin \eta' \right], \quad (12a)$$

$$\bar{y} = \frac{1}{(\omega_L/c)} \bar{\beta}_{y0} (\eta + \Delta\eta/2), \quad (12b)$$

and

$$\begin{aligned} \bar{z} = z_0 + \frac{1}{(\omega_L/c)} & \left[\bar{\beta}_1 (\eta + \Delta\eta/2) + \bar{\beta}_{x0} \int_{-\Delta\eta/2}^{\eta} \partial\eta' \left(\frac{\bar{a}}{\gamma_0} \right) \sin(\eta') \right. \\ & \left. - \int_{-\Delta\eta/2}^{\eta} \partial\eta' \left(\frac{\bar{a}^2}{4\gamma_0^2} \right) (1 - \cos(2\eta')) \right]. \end{aligned} \quad (12c)$$

The θ and ϕ components of the radiation are now

$$\begin{aligned} \frac{d^2 I_\theta}{d\omega d\Omega} \simeq \frac{e^2 \omega^2}{4\pi^2 c \omega_L^2} \left| \int_{-\Delta\eta/2}^{\Delta\eta/2} d\eta \left[\left(\bar{\beta}_{x0} \cos \theta \cos \phi + \bar{\beta}_{y0} \cos \theta \sin \phi - \left(\bar{\beta}_1 - \frac{\bar{a}^2}{4\gamma_0^2} \right) \sin \theta \right) \right. \right. \\ \left. \left. - \frac{\bar{a}}{\gamma_0} (\cos \theta \cos \phi + \bar{\beta}_{x0} \sin \theta) \sin \eta - \frac{\bar{a}^2}{4\gamma_0^2} \sin \theta \cos(2\eta) \right] \exp[i\tilde{\psi}] \right|^2, \end{aligned} \quad (13)$$

$$\frac{d^2 I_\phi}{d\omega d\Omega} \simeq \frac{e^2 \omega^2}{4\pi^2 c \omega_L^2} \left| \int_{-\Delta\eta/2}^{\Delta\eta/2} d\eta \left[(\bar{\beta}_{x0} \sin \phi - \bar{\beta}_{y0} \cos \phi) - \frac{\bar{a}}{\gamma_0} \sin \phi \sin \eta \right] \exp[i\tilde{\psi}] \right|^2, \quad (14)$$

where

$$\begin{aligned} \tilde{\psi} = \psi_0 + \frac{\omega}{\omega_L} \left[1 - (\bar{\beta}_{x0} \sin \theta \cos \phi + \bar{\beta}_{y0} \sin \theta \sin \phi + \bar{\beta}_1 (1 + \cos \theta)) \right] (\eta + \Delta\eta/2) \\ - \frac{\omega}{\omega_L} (\sin \theta \cos \phi + \bar{\beta}_{x0} (1 + \cos \theta)) \int_{-\Delta\eta/2}^{\eta} d\eta' \frac{\bar{a}}{\gamma_0} \sin \eta' \\ + \frac{\omega}{\omega_L} (1 + \cos \theta) \int_{-\Delta\eta/2}^{\eta} d\eta' \frac{\bar{a}^2}{4\gamma_0^2} \\ - \frac{\omega}{\omega_L} (1 + \cos \theta) \int_{-\Delta\eta/2}^{\eta} d\eta' \frac{\bar{a}^2}{4\gamma_0^2} \cos(2\eta') \end{aligned} \quad (15)$$

is the phase and $\psi_0 = -(\omega/\omega_L)\Delta\eta/2 - (\omega/c)z_0(1 + \cos \theta)$.

The integral in Eq. (15) may be evaluated to obtain

$$\tilde{\psi} \simeq \psi_0 + d_0 \eta + d_x \cos \eta + d_z \sin(2\eta), \quad (16)$$

where

$$d_0 = \frac{\omega}{\omega_L} \left\{ 1 + \left[-(\bar{\beta}_{x0} \cos \phi + \bar{\beta}_{y0} \sin \phi) \sin \theta - \left(\bar{\beta}_1 - \frac{\bar{a}^2}{4\gamma_0^2} \right) (1 + \cos \theta) \right] \right\}, \quad (17a)$$

$$d_x = \frac{\omega}{\omega_L} [\sin \theta \cos \phi + \bar{\beta}_{x0} (1 + \cos \theta)] \frac{\bar{a}}{\gamma_0}, \quad (17b)$$

and

$$d_z = -\frac{\omega}{\omega_L} (1 + \cos \theta) \frac{\bar{a}^2}{8\gamma_0^2}. \quad (17c)$$

Substituting (16) into (13) and (14), we obtain

$$\frac{d^2 I_\theta}{d\omega d\Omega} \simeq \frac{e^2 \omega^2}{4\pi^2 c \omega_L^2} \left| \left[g_{0,\theta} I_0 - \frac{\bar{a}}{\gamma_0} I_x (\cos \theta \cos \phi + \bar{\beta}_{x0} \sin \theta) - \frac{\bar{a}^2}{4\gamma_0^2} I_x \sin \theta \right] \right|^2, \quad (18)$$

$$\frac{d^2 I_\phi}{d\omega d\Omega} \simeq \frac{e^2 \omega^2}{4\pi^2 c \omega_L^2} \left| \left[g_{0,\phi} I_0 + \frac{\bar{a}}{\gamma_0} I_z \sin \phi \right] \right|^2, \quad (19)$$

where

$$I_0 = \int_{-\Delta\eta/2}^{\Delta\eta/2} d\eta' \exp[i\tilde{\psi}(\mathbf{x}_0, \underline{\beta}_0, \eta')], \quad (20a)$$

$$I_x = \int_{-\Delta\eta/2}^{\Delta\eta/2} d\eta' \sin \eta' \exp[i\tilde{\psi}(\mathbf{x}_0, \underline{\beta}_0, \eta')], \quad (20b)$$

$$I_z = \int_{-\Delta\eta/2}^{\Delta\eta/2} d\eta' \cos(2\eta') \exp[i\tilde{\psi}(\mathbf{x}_0, \underline{\beta}_0, \eta')], \quad (20c)$$

$$g_{0,\theta} = (\bar{\beta}_{x0} \cos \phi + \bar{\beta}_{y0} \sin \phi) \cos \theta - \left(\bar{\beta}_1 - \frac{\bar{a}^2}{4\gamma_0^2} \right) \sin \theta, \quad (21a)$$

and

$$g_{0,\phi} = \bar{\beta}_{x0} \sin \phi - \bar{\beta}_{y0} \cos \phi. \quad (21b)$$

Now, we will integrate over η by expanding the exponential of $\sin \eta$ and $\cos \eta$ in terms of Bessel functions

$$\exp[id_z \sin 2\eta] = \sum_{m=-\infty}^{\infty} J_m(d_z) \exp[i2m\eta], \quad (22)$$

$$\exp[id_z \cos \eta] = \sum_{n=-\infty}^{\infty} J_n(d_z) \exp[in(\pi/2 + \eta)] = \sum_{n=-\infty}^{\infty} i^n J_n(d_z) \exp[in\eta]. \quad (23)$$

Substitute Eqs. (22) and (23) into Eqs. (20a)-(20c), we obtain

$$I_0 = 2e^{i\psi_0} \sum_m J_m(d_z) \sum_\ell i^\ell J_\ell(d_z) p_{\ell,m}, \quad (24a)$$

$$I_x = -e^{i\psi_0} \sum_m J_m(d_z) \sum_\ell i^\ell [J_{\ell-1}(d_z) + J_{\ell+1}(d_z)] p_{\ell,m}, \quad (24b)$$

$$I_z = -e^{i\psi_0} \sum_m J_m(d_z) \sum_\ell i^\ell [J_{\ell-2}(d_z) + J_{\ell+2}(d_z)] p_{\ell,m}, \quad (24c)$$

$$p_{\ell,m} = \frac{1}{2i(2m + \ell + d_0)} \left(e^{i[(2m+\ell+d_0)\Delta\eta/2]} - e^{-i[(2m+\ell+d_0)\Delta\eta/2]} \right). \quad (24d)$$

III. Fundamental and Harmonics

The emission on axis is peaked at the fundamental and harmonic frequencies, which can be obtained from $p_{\ell,m}$

$$p_{\ell,m} = \pi N_o \frac{\sin \chi}{\chi},$$

where $\chi = (2m + \ell + d_0)(\pi N_o)$. Since $p_{\ell,m}$ is peaked at $\chi = 0$. The frequencies of the on axis radiation associated with the peak intensity are

$$\omega_h = h\omega_L \frac{4\gamma_0^2}{1 + a^2/2 + \gamma_0^2(\beta_{x0}^2 + \beta_{y0}^2)}, \quad (25)$$

where $h = -2m - \ell$ is the harmonic number.

The expressions for I_0 , I_x and I_z , written in terms of the harmonic number, become

$$I_0 = 2e^{i\psi_0} \sum_{h=1}^{\infty} i^h p_h \sum_m (-1)^m J_m(d_z) J_{h+2m}(d_z) \quad (26a)$$

$$I_x = -e^{i\psi_0} \sum_{h=1}^{\infty} i^h p_h \sum_m (-1)^m J_m(d_z) [J_{h+2m-1}(d_z) + J_{h+2m+1}(d_z)] \quad (26b)$$

$$I_z = -e^{i\psi_0} \sum_{h=1}^{\infty} i^h p_h \sum_m (-1)^m J_m(d_z) [J_{h+2m-2}(d_z) + J_{h+2m+2}(d_z)], \quad (26c)$$

$$p_h = \pi N_o \frac{\sin \chi_h}{\chi_h}, \quad (26d)$$

where $\chi_h = (d_0 - h)\pi N_o$.

The analytical expression for the radiated energy per unit solid angle per unit frequency per electron, given by the sum of the expressions (18) and (19), with definitions given by (17a-c), (21a-b) and (26a-d), are valid for a large range of values of laser amplitudes. For $a \ll 1$, only fundamental radiation will be observed. Intensity of harmonic radiation becomes important for $a > 1$.

The spectrum width of a single radiating electron is

$$\delta\omega_h/\omega_h \simeq \frac{1}{N_o},$$

obtained by equating $\chi_h = \pi$. Since the laser pulse typically has a large number of periods, the spectral width of the radiation, in principle, could be very narrow. However, the spectral width will be determined by the energy spread and the emittance of the electron beams.

IV. Numerical Results and Comments

In this section we present numerical results for the energy radiated per unit solid angle per unit frequency per electron. Two examples are given: 1) no transverse beam velocity and 2) transverse velocity $\beta_{x0} = 0.0075$. In both cases, the electron beam has $\gamma_0 = 80$. The normalized laser amplitude is $a = 3.2 \times 10^{-2}$ and the number of periods in the laser pulse is taken to be 20. The small number of periods is not typical for a laser pulse, but it illustrates the principles, while avoiding difficulties in displaying data with very narrow line widths.

For the electron beam without initial transverse velocity, the backscattered radiation is peaked on axis. Figure 2 is a plot of the energy radiated as a function of frequency and angle θ (evaluated in the $\phi = 0$ plane), where ω_1 is the frequency of the fundamental based on Eq. (25). The bandwidth should be 5%, and this is confirmed by Fig. 3, which is obtained on axis. The solid curve in Fig. 4 is a plot of the peak energy radiated for each given angle θ . As expected the radiation is confined within an angle less than $1/\gamma_0$. The dashed curve in Fig. 4 is the corresponding frequency.

Realistic electron beams have finite emittance. If the electron beam has an initial transverse velocity, the radiation pattern is distorted. Figure 5 is a plot of the energy radiated as a function of frequency and angle θ (evaluated in the $\phi = 0$ plane), for $\beta_{x0} = 0.0075$. A plot of the energy radiated on axis as a function of the normalized frequency, shown in Fig. 6, shows that the radiation field on axis is reduced by about 25% as predicted by the analytical expression. The solid curve in Fig. 7 is the plot of peak energy radiated for each given angle θ and the dashed curve in Fig. 7 is the corresponding frequency. The peak frequency is at angle $\theta \simeq \beta_{x0}$, while the peak of the intensity is at a smaller angle.

We have derived an analytic expression for the intensity distribution of Thomson scattered radiation for the case of a linearly polarized laser pulse incident on a counterpropagating electron beam. We have calculated the effects of small initial transverse momentum, including the distortion of the intensity distribution, the reduction in on-axis intensity, and the increase in bandwidth. We are currently extending this work to consider the effects of emittance (for a distribution of electrons) and laser pulse shape on the scattered radiation.

Acknowledgements

This work is supported by the Medical Free Electron Laser Program of ONR.

References

1. E. S. Sarachik and G. T. Schappert, Phys. Rev. **D1**, 2738 (1970).
2. M. A. Piestrup, G. E. Rothbart, R. N. Fleming and R. H. Pantell, J. Appl. Phys. **46**, 132 (1975).
3. A. Luccio and B. A. Brill, US Pat #4,598,415, dated July 1, 1986.
4. F. E. Carroll, et al., Investigative Radiology **25**, 465 (1990).
5. P. Sprangle, A. Ting, E. Esarey and A. Fisher, submitted for publication.
6. E. Esarey, P. Sprangle, A. Ting and S. K. Ride, submitted to the 1992 FEL Conf.
7. W. B. Colson, "Free Electron Laser Theory", Ph.D. Thesis, Stanford University, 1977.
8. S. K. Ride and W. B. Colson, Stanford University High Energy Physics Lab Report 858 (1979).
9. W. B. Colson, IEEE J. Quantum Electron **QE-17**, 1417 (1981).
10. W. B. Colson, G. Dattoli and F. Ciocci, Phys. Rev. A **31**, 828 (1985).
11. R. Barbini, F. Ciocci, G. Dattoli and L. Giannessi, Nuovo Cimento **13**, 1 (1990).
12. C. A. Br , presented at the 1992 FEL Conf.
13. P. Sprangle and E. Esarey, Phys. Fluids B **4**, 2241 (1992).
14. W. B. Colson and S. K. Ride, J. of Appl. Phys. **20**, 61 (1979).
15. P. Sprangle, L. Vlahos and C. M. Tang, IEEE Trans. on Nuclear Sci. **NS-30**, 3177 (1983).
16. E. Esarey and S.K. Ride and P. Sprangle, private communications.

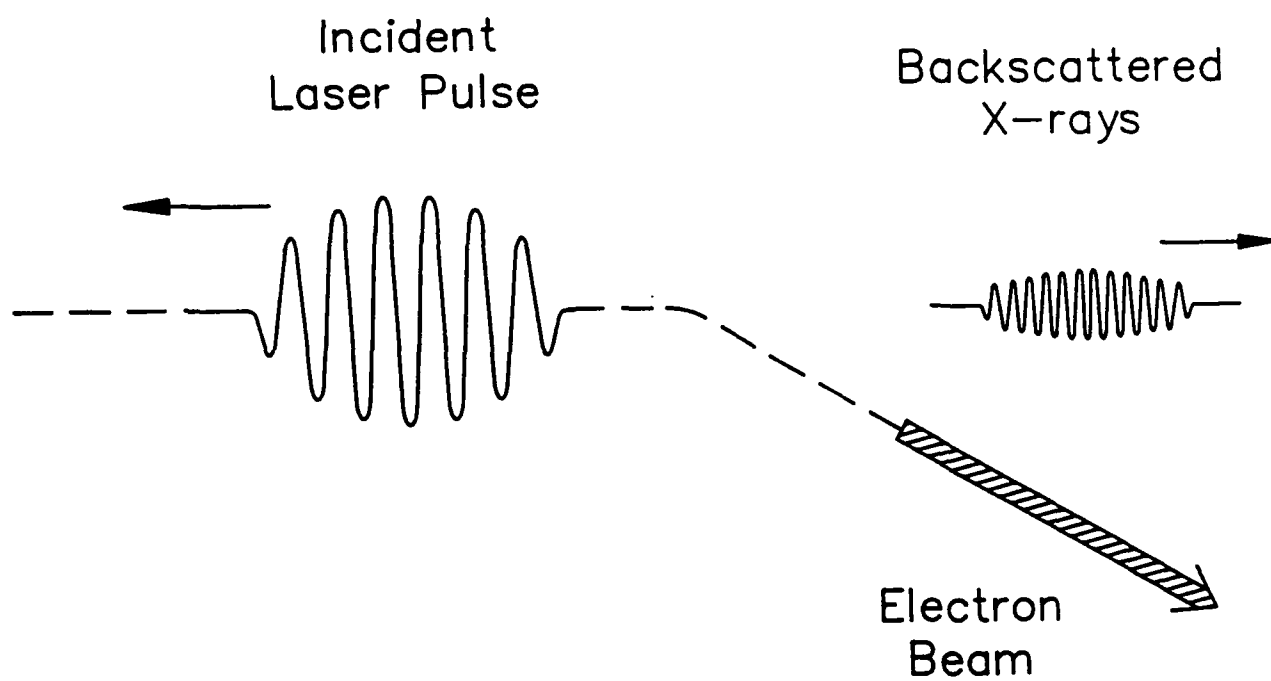


Fig. 1. Schematic of the Thomson backscatter configuration intercepts an incoming laser pulse.

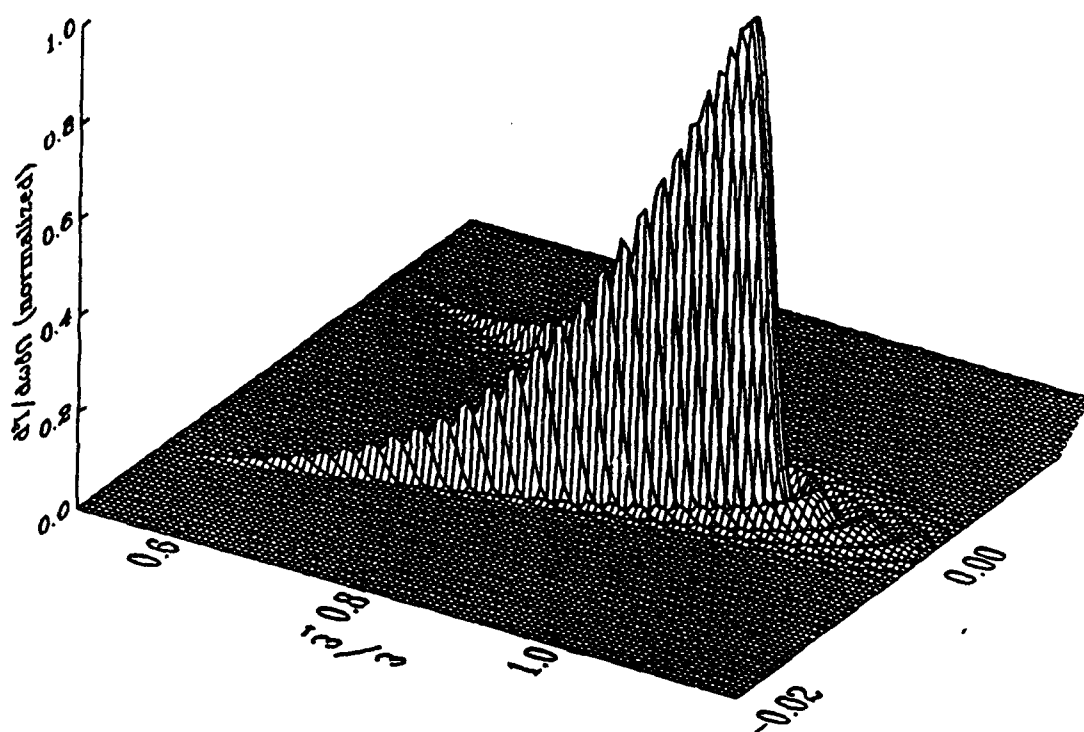


Fig. 2. Plot of normalized energy radiated per unit solid angle per unit frequency per electron as a function of normalized frequency and angle θ (evaluated in the $\phi = 0$ plane) for an electron with no initial transverse velocity.

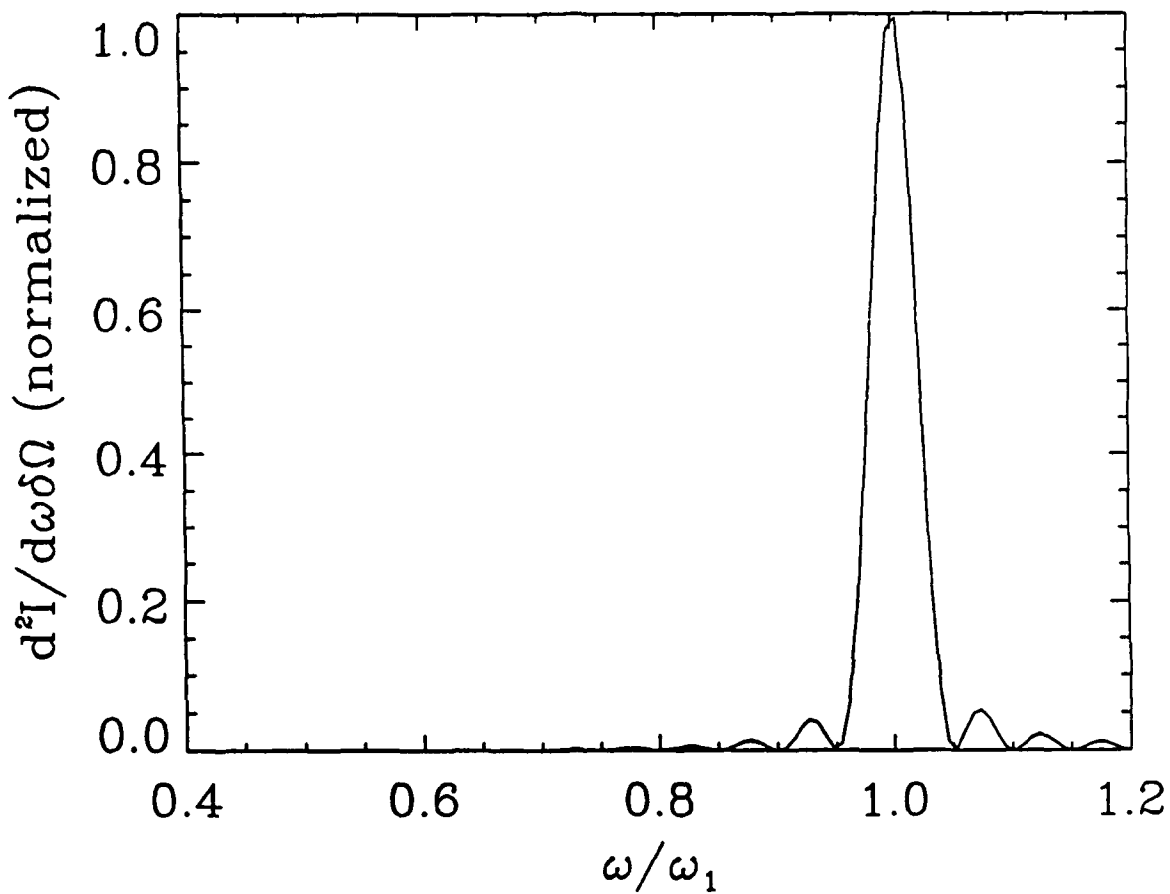


Fig. 3. Plot of normalized energy radiated on axis per unit solid angle per unit frequency per electron as a function of normalized frequency.

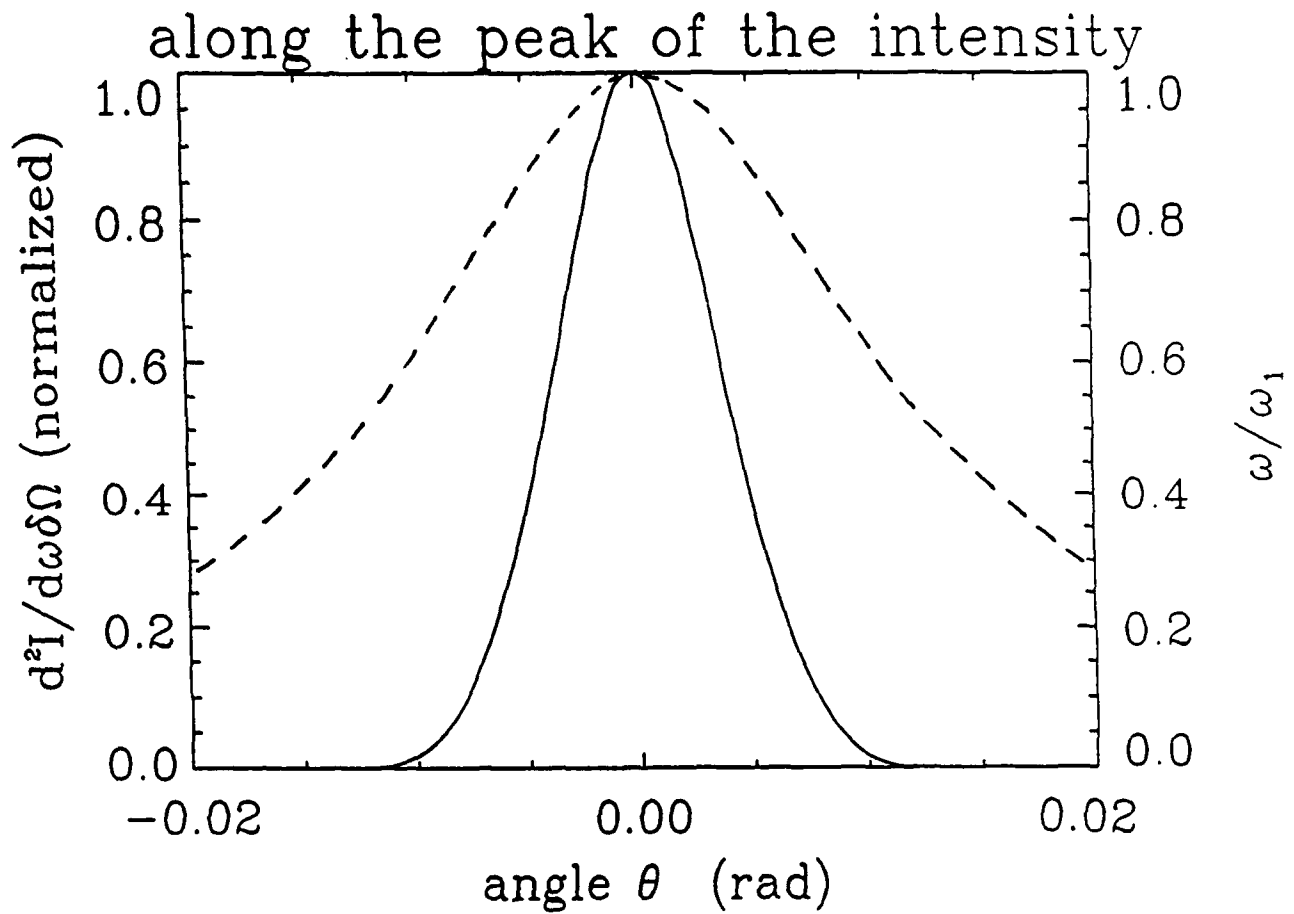


Fig. 4. Plot of the peak energy radiated (solid curve) and the corresponding frequency (dashed curve) for each given angle θ (evaluated in the $\phi = 0$ plane).

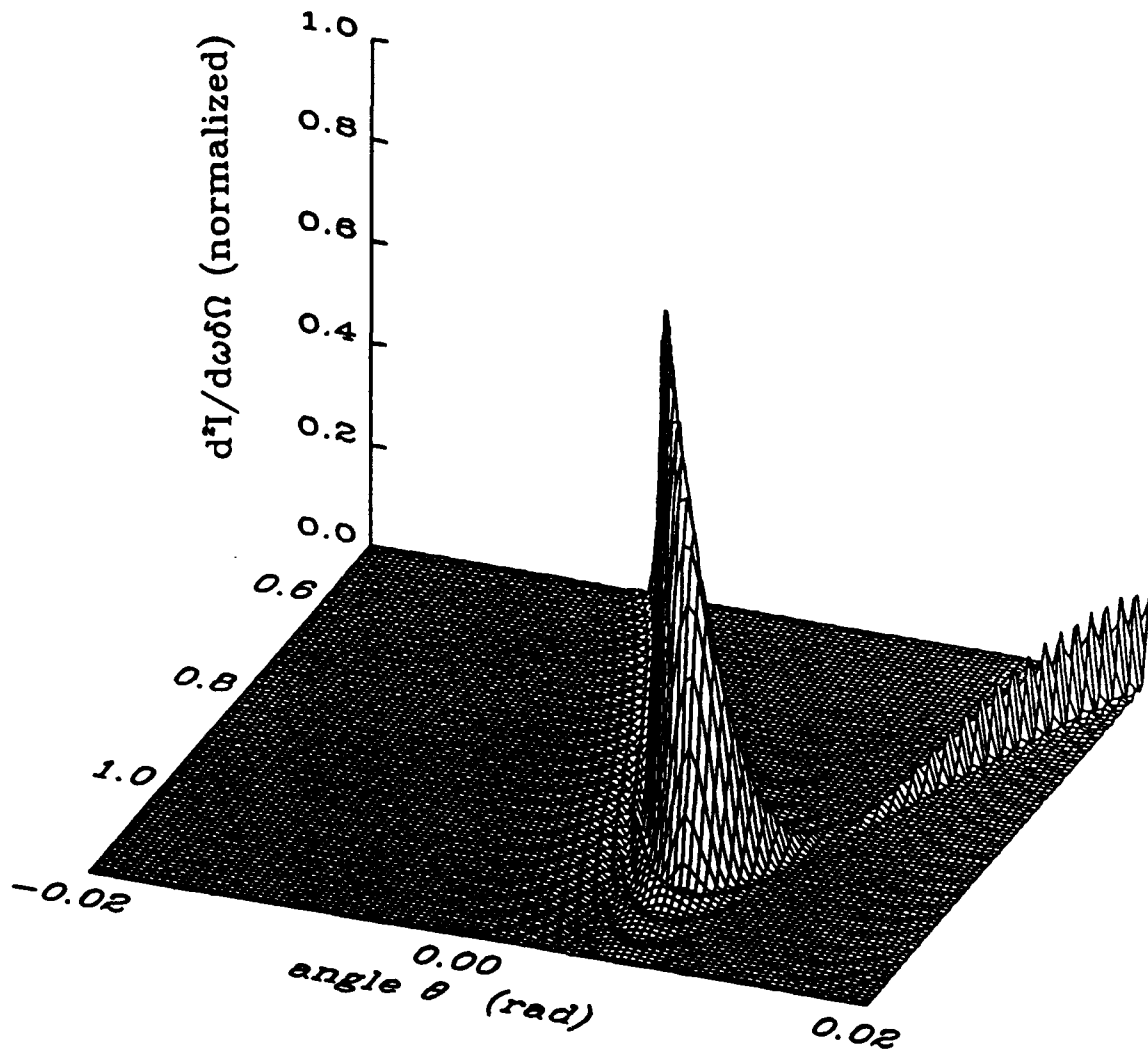


Fig. 5. Plot of normalized energy radiated per unit solid angle per unit frequency per electron as a function of normalized frequency and angle θ (evaluated in the $\phi = 0$ plane) for an electron with $\beta_{e0} = 0.0075c$.

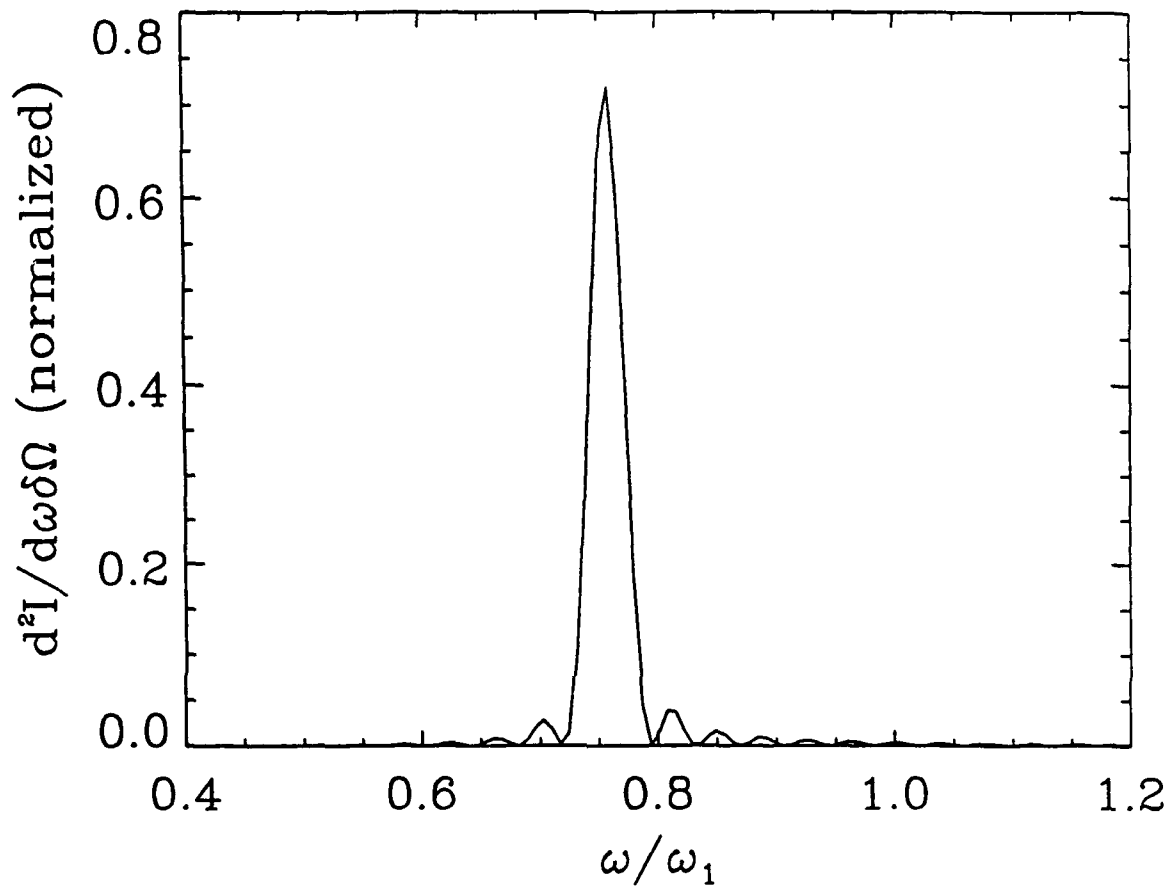


Fig. 6. Plot of normalized energy radiated on axis per unit solid angle per unit frequency per electron as a function of normalized frequency.

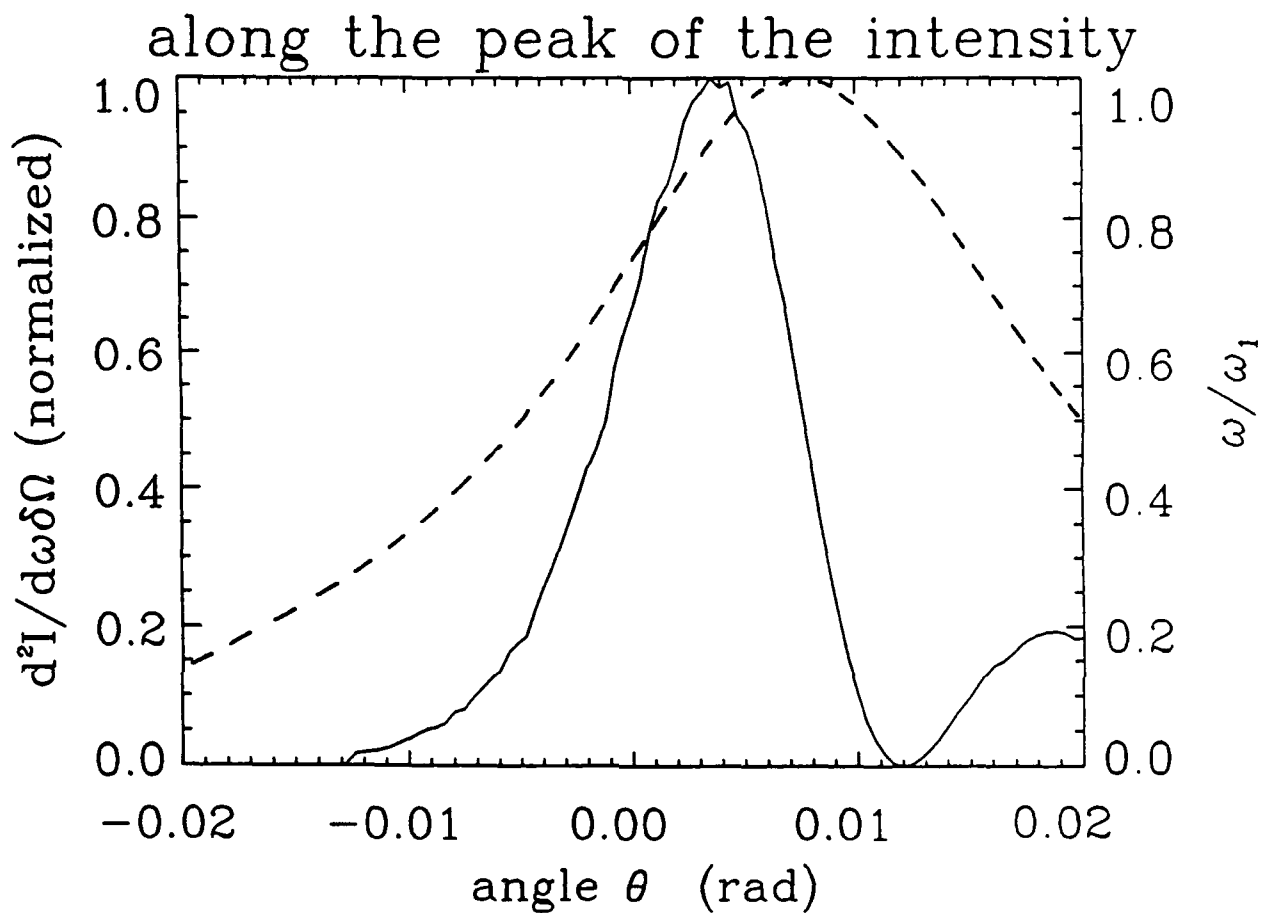


Fig. 7. Plot of the peak energy radiated (solid curve) and the corresponding frequency (dashed curve) for each given angle θ (evaluated in the $\phi = 0$ plane).